HIGH THRUST DENSITY ELECTRIC PROPULSION FOR HEAVY PAYLOAD IN-SPACE TRANSPORTATION

Monika Auweter-Kurtz[1] and Helmut Kurtz[2]

[1]Institut of Space Systems (IRS), Universität Stuttgart, Pfaffenwaldring 31, 70550 Stuttgart, Germany, Tel. +49(0)711-685-2378, Fax: +49(0)711-685-7527, Email: auweter@irs.uni-stuttgart.de,
[2]Institut of Space Systems (IRS), Universität Stuttgart, Pfaffenwaldring 31, 70550 Stuttgart, Germany, Tel. +49(0)711-685-2389, Fax: +49(0)711-685-7527, Email: kurtz@irs.uni-stuttgart.de

ABSTRACT

Mission studies for a crewed Mars mission clearly show that with chemical propulsion the trip times are too long and the propellant mass is very high. For these kinds of missions stationary, electric thrusters are preferable because of their high thrust levels and high specific impulse. In view of this, thermal arcjets, MPD self-field and MPD applied-field thrusters and, most recently, hybrid thrusters have been developed in the US, Russia and in Germany at the Institute of Space Systems (IRS) of the Universität Stuttgart. Based on a brief review of the state of the art of stationary high power thermal and MPD arcjets and hybrid thrusters, future development needs and trends are presented in this publication.

1. INTRODUCTION

Mission scenarios such as building a scientific outpost on the moon or human exploration of Mars require new propulsion systems for in-space transportation of heavy payloads. [1] A thrust level of at least 100 N and a specific impulse level of 30 km/s are of central im-portance to increase the payload capacity and shorten the trip time as much as possible. The propulsion sys-tem mass should be as lightweight as possible.

Therefore, both the thrust density and efficiency of the propulsion device should be high. Nuclear and solar thermal propulsion offer high thrust densities but are weak in their specific enthalpy level which is clearly below 10 km/s (see Table 1). Ion and Hallion thrusters offer both the required exit velocity level but their thrust density is far too low.

Promising in-space propulsion candidates for heavy payloads are currently thermal arcjet thrusters with which an exit velocity of 20 km/s at 100 kW and a thrust density of more than 2100 N/m^2 can already be achieved. This technology is in an advanced develop-mental stage; low power devices have been imple-mented in commercial applications with hydrazine as propellant and are exceptionally reliable. The highest thrusts and thrust densities reached to date have been achieved with MPD self-field thrusters.

Table 1: Performance data of a solar thermal rocket [2], a nuclear thermal rocket NERVA [3], a high power thermal arcjet HIPARC [4], a self-field MPD thruster DT2 [5], an applied-field MPD thrusters [6], ion propulsion system DS1 [7], a Hallion thruster SPT 100 [10] and two hybrid concepts ATTILA [8] and VASIMR [9] with the Saturn V (1 stage S-IC, rocket type-F-1) as reference.

	Thrust F [N]	Exhaust velocity c_e [km/s]	Nozzle exit area A [m^2]	Thrust density [N/m^2]
Saturn V	7600000	<5	10.752	706839
Solar Thermal	25	<8	0.002	12732
Nuclear Thermal	340000	<8	11.282	30138
Thermal Arcjet	6	20	0.003	2122
MPD Self-Field	28	<15	0.008	3565
MPD A-F	4.50	42	0.020	225
Ion Propulsion	0.092	<60	0.071	1302
Hall-Ion Thruster	0.10	<30	0.008	12732
VASIMR	0.006?	20?	0.003	2?
Thermal-Inductive Hybrid (ATTILA)	35?	7?	0.003	10548?

However, the effective exit velocity is still limited to 15 km/s.

Proc. '4th Int. Spacecraft Propulsion Conference', Cagliari, Sardinia, Italy 2-4 June 2004 (ESA SP-555, October 2004)

Although the achievable thrust density is an order of magnitude lower, applied-field MPD thrusters should be considered for this type of application because it is possible to achieve very high exit velocities. Hybrid thrusters are also an interesting development, but they have not been investigated very extensively yet. The hybrid concept ATTILA, in which a thermal arcjet thruster is combined with a second inductive stage, is remarkable for its high thrust densities. A significant increase in the effective exit velocities of these devices compared to the thermal arcjet thrusters can be expected.

All of these high power, high thrust density thrusters are still at a relatively rudimentary development stage and are far from being able to be used in space. Up to now, mostly basic investigations have been performed and some tools for the construction have been developed. A systematic investigation and optimization of these technologies is still outstanding. Appropriate developmental test facilities are necessary in some cases. Following is a description of the developmental stage of these stationary operated thrusters and of future development needs.

2. THERMAL ARCJETS

In the last two decades, electrothermal arcjets have been investigated in a wide power range (0.1kW to 100 kW) for a wide range of uses. [11, 12] Low power arcjet thrusters from General Dynamics (Primex), USA, have been used since 1993 as North-South-Station-Keeping (NSSK) thrusters with hydrazine as propellant [13], and were foreseen as primary propulsion for the AMSAT P3 satellite with ammonia as propellant (ATOS). [11] The medium power ammonia arcjet thruster on the USAF Argos satellite, the ESEX experiment [14], also of Primex origin, proved the feasibility of such a thruster for orbit transfer. In the area of high electric power up to approximately 100 kW, an operable laboratory model for hydrogen as propellant has been developed [4] and the potential for this kind of technology has been investigated.

In an arcjet thruster, electric power from an external power source is used to heat a propellant gas with an electric arc. The heated gas expands through a converging-diverging nozzle to produce thrust. The thruster is rotational-symmetric, with a central cathode normally made of a tungsten alloy (1-2% ThO_2) and the nozzle, also from refractory materials, switched as anode. The gas flows through this inner-electrode region and the arc is heated by Ohmic heat and is at least partially dissociated and ionized.

The power supply system is a key component in operational arcjet systems. It has to assure reliable arc initiation and a stable steady state operation. The arc is ignited by a series of high voltage (> 2 kV) pulses across the arcjet electrodes. This generates sparks in the propellant gas which leads the way for the main discharge. The power control unit (PCU) has to take over the discharge by means of a fast control unit while maintaining a stable discharge and withstanding possible discharge instabilities, which are mainly caused by erratic arc attachments.

In the last few years, immense progress has been made in mass savings for the power supply for low power arcjets, mainly by the application of modern digital electronics, which lead to PCU efficiencies between 90 and 95%.

Efficiency

The main losses in arcjet propulsion are frozen flow losses. Since the residence time of the propellant in the nozzle is in the order of 1 µs, the energy comprised in dissociation, ionization and excitation cannot be recovered in the nozzle. Therefore, the efficiencies of arcjets with molecular gases are restricted to $\eta < 50\%$, as an example see Fig. 1.

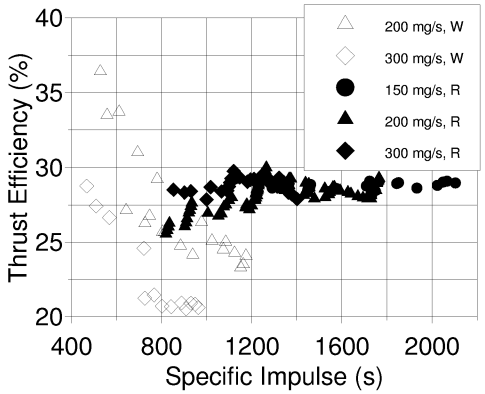

Fig. 1. Exemplarily efficiency/I_{sp} curve for HIPARC, water-cooled (W) and radiation-cooled (R) version, with hydrogen as propellant [4].

There are only few means to increase the efficiency:

- Regenerative cooling: With regenerative cooling, the propellant is led through the hottest parts of the thruster. Part of the thermal losses can be recovered and the efficiency raised. The gain in η naturally depends on the heat capacity of the propellant, i.e. c_p and mass flow and the ΔT. From the prospective propellants, H_2 is the best suited. Its c_p is more than five times higher than that of NH_3 (both at 1000 K). Hydrogen can remove about 2.9 x 107 J/kg during heating (by $\Delta T \approx 2000$ K). Assuming for example

$$\frac{regen.cooling\ power}{input\ power} = \frac{2\eta\,\Delta h_{RC}}{c_e^2}$$

an arcjet in the 10 km/s c_e regime with > 40% efficiency, the above ratio becomes > 23%. An extra advantage of regenerative cooling consists in reducing

the extreme heat stresses near the arc attachment area and nozzle throat and hence prolonging the lifetime of the thruster.

- Bi-exit or dual-cone nozzle: Primex [15] and Aston [16] suggested the bi-exit anode to recover some of the frozen flow losses. The idea is to pro-vide an area of relatively high density and sufficient time to achieve some recombination. This could be achieved by a dual-cone anode, the diverging part of the noz-zle being separated into two regions: the first one has a slowly varying area allowing some recombine-tion, the second one is a normal diverging nozzle for rapid expansion.

For introducing power into the arc, the current should be as low as possible to alleviate the heat loads to the electrodes, meaning the discharge voltage has to be high. An arcjet thruster system is normally current con-trolled. The discharge voltage results from and is determined by several factors:

- *propellant*: monoatomic gases with low dissociation potential such as argon show the lowest voltage at constant current, H_2 the highest
- *mass flow*: the discharge voltage rises with rising mass flow
- *constrictor length*: the length of the constrictor, i.e. the length of the arc, determines the voltage drop due to the Ohmic losses
- *constrictor diameter*: at constant mass flow and current the voltage is lower with larger constrictor diameter (lower plenum pressure)

Influence of Propellants

Arcjets can operate on a variety of propellants. The molecular mass of the propellant should be as low as possible for achieving a high specific impulse. On the other hand, the propellant and/or the dissociated products may not react chemically with the thruster body and electrode materials. This excludes all compounds containing either oxygen or carbon. Compounds containing elements which could be deposited on the spacecraft should also be ruled out. This restricts the preferred choice to H_2 and hydrogen/nitrogen compounds. Another advantage of H_2 is the higher discharge voltages, which help relay power to the propellant at low discharge currents.

Hydrazine is already in use for low power arcjet applications. The hydrazine has to be gasified in a decomposer, yielding a mixture of hydrogen, nitrogen and a small amount of ammonia. The I_{sp} is limited from 500 s for small arcjets (< 1 kW) to more than 650 s for medium-size arcjets (ca 2 kW). Efficiencies lie between 30% at high I_{sp} and 40% at ca 500 s.

Ammonia represents space qualified technology already in use on ESEX and ATOS. The I_{sp} is limited from 500 s for small arcjets (< 1 kW) to about 900 s extrapolated for medium-size arcjets (> 30 kW). Efficiencies lie in the order of 30-40%.

Hydrogen is the best choice for arcjets regarding the I_{sp} because of the low atomic mass and its good thermophysical properties. Because of the frozen flow losses, the efficiencies are low, about 25 to 40%, but they can be raised by proper designs, especially those including regenerative cooling. The maximum I_{sp} depends on the size of the thruster: with about 1 kW ca. 1000 s, with 10 kW ca. 1500 s and with 100 kW over 2000 s, see Fig. 2. A disadvantage of hydrogen is the storage, which has to be in liquid form. But because a lot of progress has been made, for high power missions this issue seems to be of minor concern.

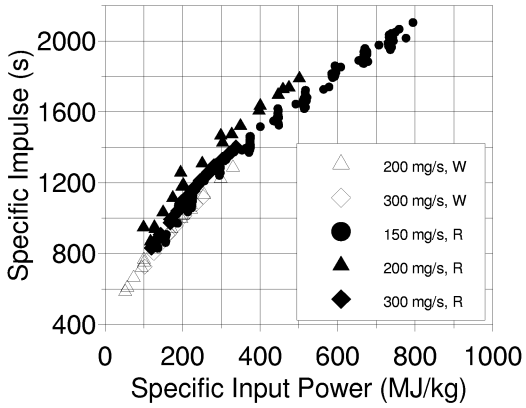

Fig. 2. Specific impulse vs. specific power for a radiation-cooled (R) and a water-cooled (W) high power arcjet thruster. [4]

For electrical orbit transfer vehicles (EOTV) a tank fraction of 0.15 has been estimated [12] which would yield mass savings of 43% for a 2000-kg S/C for a LEO to GEO transfer mission when the solar panels are attributed to the EOTV. This applies to an I_{sp} of 1200 s, a 30-kW engine and 200 d transfer time. The system conceived eliminates long term cryogenic storage re-quirements by utilizing the hydrogen boil-off.

Qualification Advantages

In comparison with the other electric propulsion types, such as ion, Hall-ion, and applied-field MPD thrusters, the qualification requirements are much less demanding. The PCU is simpler. Beside the ignition pulse only one power circuit is needed at relatively low (80-200 V) voltages. The physics of arcjets allow representative operation at tank pressure levels in the range of 1-10 Pa, allowing the use of roots-pump systems, a vacuum level about a factor of 1000 less demanding than with ion or SPT thrusters. Due to the high thrust levels, the accumulated test time is also about a factor 10 smaller than with the above mentioned thruster types.

3. MAGNETOPLASMADYNAMIC THRUSTERS

The main operating principle of MPD thrusters is to use the electromagnetic forces to accelerate the propellant. Ohmic heating and the resulting thermal thrust portion play a subordinate role but often one that should not be ignored.

Generally, two main types are spoken of:

self-field MPD thrusters

applied-field MPD thrusters.

MPD applied-field thrusters are always operated in a stationary mode. Self-field thrusters have three operating modes: continual, quasi-stationary and non-stationary. Because from today's point of view high average thrust can only be achieved with stationary MPD self-field accelerators, only this type of thruster will be considered.

When designing MPD thrusters, one must be aware that only charged particles can be accelerated by electromagnetic force. Therefore, the propellant should be almost completely ionized in order to achieve high efficiency. A recombination is undesirable in the entire thruster. Therefore, the gas temperatures in MPD devices are higher and the pressure is lower than in thermal arcjet devices. The pressure in the discharge chamber is typically between $5 \cdot 10^{-4}$ bar and 0.5 bar.

3.1 Self-Field (SF-MPD) Thrusters

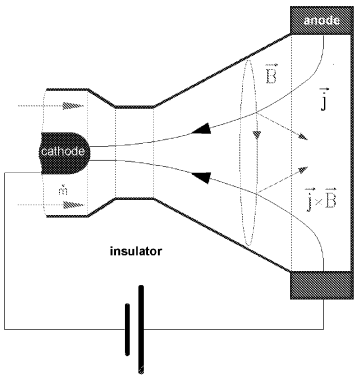

Fig. 3. Operating principle of the self-field MPD thruster.

The SF-MPD thrusters (Fig. 3) have been extensively investigated experimentally and numerically, both with continuous and with pulsed quasi-steady operation, with many different propellants. The principle of operation should be clear from Fig. 4 showing how the self-induced circumferential magnetic field (B_θ) interacting with the applied meridional currents produce meridional forces on the plasma normal to the current, mostly axially and radially inward. These forces result in direct acceleration, pressure ("pinch" pressure) and temperature rise with subsequent expansive acceleration, respectively [18, 19].

Of the thruster types discussed here, the SF-MPD thrusters have the lowest arc volt-ages for a given power level be-cause the self-induced magnetic fields are relatively weak unless very high currents (tens of kiloamps) are applied. Typical values (for nozzle-type thrusters with argon as propellant) are ≈ 50-70 V for a ≈ 200 kW continuous thruster. Since the electrode loss voltages change much less rapidly with the current or power level, the thermal efficiencies of these thrusters improve with increasing power. Because of the high currents required, the SF-MPD thrusters also have the most severe electrode erosion and cooling problems.

For the in-space transportation missions considered here only continuous operating thrusters make sense. By directly comparing geometrically identical thrusters in continuous operating mode to quasi-steady pulsed mode [20], it could be shown that results of q-s thrusters could not be extrapolated to the steady operation case and most q-s results are therefore irrelevant for real high power thrust missions.

Especially if the thruster is nozzle shaped, a not to be neglected part of electrothermal thrust is added to the pure MPD thrust. Thrust vs. current curves for various argon mass flow rates for the IRS DT-2 thruster, Fig. 4,

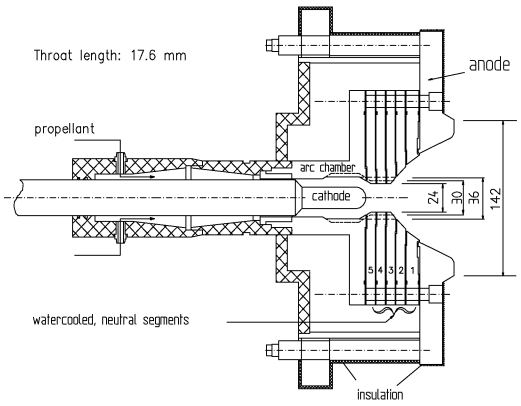

Fig. 4. Nozzle type MPD thruster DT (DT2 with 24 mm throat , DT6 with 36 mm).

are shown in **Fig. 5**. Also plotted in this graph is the pure electromagnetic thrust, calculated according to [18, 19]

$$T_M = \frac{\mu_0}{4\pi} I^2 \left(\ln \frac{r_a}{r_c} + \frac{3}{4} \right). \qquad (1)$$

$T_{m,max}$ and $T_{m,min}$ are calculated with cathode radius r_c and for the maximum and minimum possible anode radius r_a. It can be seen that at lower current levels the electrothermal part of the thrust is prevalent and only with rising current levels does the total thrust approach the gradient angle of the magnetic thrust.

Empirically, it has been known for some time that the current-to-gas-mass flow ratio $I^2/\dot{m}$ has a limit for each thruster and propellant where stable operation of

the arc becomes impracticable. Beyond that so-called "onset" value, pronounced arc voltage fluctuations, severe anode spots and anode erosion, increased anode losses and thruster efficiency drop are observed. These instabilities were investigated and discussed in detail in at different institutes [interalia 21, 22, 23, 24, 25, 27].

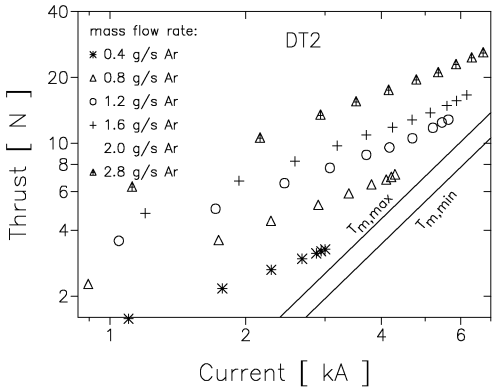

Fig. 5 Thrust vs. current curves for the DT2 thruster at various mass flow rates.

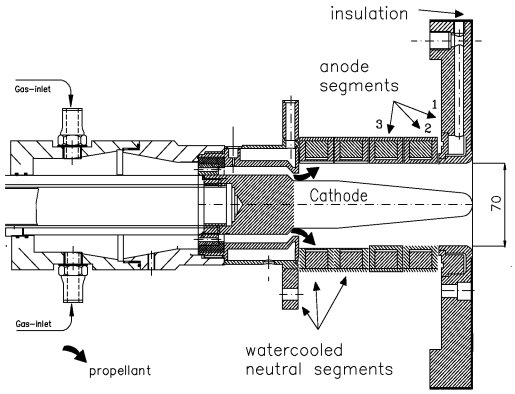

Fig. 6. Scheme of the ZT3 thruster of the IRS.

Some of these studies indicate that a change of geometry from a nozzle type to a cylindrical device should allow for higher specific impulses.

Extended cathodes and long cylindrical anodes have been designed and operated by IRS in steady-state mode, the ZT thruster series, to counteract anode starvation due to pinch forces which would not occur with a purely radial current flow.

The cylindrical ZT3, shown in Fig. 7, consists of three anode segments, two neutral segments and a backplate, all out of water-cooled copper, and the thoriated tungsten cathode. The cathode was designed to counterbalance thermal damage effects encountered at high current levels (see below). In the back the anode diameter is 40 mm, and is subsequently reduced to a 10 mm radius at the tip.

In Fig. 7 experimental results of the ZT3 thruster with a mass flow rate of 2 g/s argon are compared to the results of the nozzle shaped thruster DT6 with 36mm throat diameter, both running at the same mass flow rate. This comparison shows that the voltage of the cylindrical thruster is low and increases only slowly with the current, while for the nozzle shaped thruster it is a factor two to four times higher and rises steeply. At ca 7450 A plasma instabilities occur for the DT6, also recognizable by the additional ascent of the voltage. For the ZT3 thruster, no indication of an occurrence of instabilities could be detected up to 12700 A where an $I^2/\dot{m}$ value of more than 8×10^{10} A^2s/kg was reached, whereas for the nozzle type MPD thruster a critical $I^2/\dot{m}$ value of ca 2.7×10^{10} A^2s/kg was found.

With the ZT3 the thrust increases with current and reaches ca 10 N at 12.7 kA.

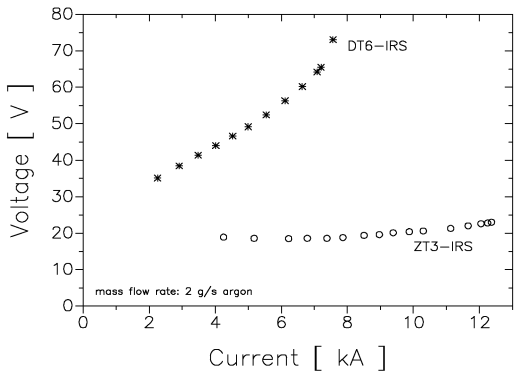

Fig. 7. Voltage-current characteristics of the ZT3 and DT6 thrusters.

Through such geometric variations, found mostly empirically, but partly also by model calculations [28], considerable performance improvements have been achieved. It has been shown that the onset limits and thereby also the achievable specific impulse and efficiency values depend very strongly on the thruster geometry, the propellant used and on the absolute thruster size, the power level and operating regime relative to the thruster size.

In summary, continuous water-cooled self-field thrusters have, under reliable test conditions (adequate vacuum), reached efficiencies with argon of up to ≈ 25% at I_{sp} values of about 1400 s, at power levels up to ≈ 500 kW. The low efficiencies are due to low arc voltages, compared to those of thermal arcjet thrusters and low thermal efficiencies (55 to 80%). Radiation-cooled SF thrusters should have higher thermal efficiencies but are mostly of lower power level.

For pulsed SF-MPD thrusters at power levels of 3 to 6 MW, efficiencies into the mid-thirties at I_{sp} levels of 2000 to 3000 s and correspondingly much higher voltages and thermal efficiencies have been reported for argon, but it is very doubtful if these values could be reached by continuous running SF-MPD thrusters.

Electrode Design. An understanding of the electrode arc attachment regions is essential for successful thruster design and operation in view of the following problems:

- electrode erosion, which is critical both for thruster life and for spacecraft surface contamination;
- transition from uniform to spot attachment on the anodes which limits the performance (I_{sp} and η) and causes both excessive erosion and electromagnetic noise (EMI);
- electrode losses, which critically affect thruster efficiency and cooling requirements (i.e. thruster weight).

Erosion of cathodes is not an issue from the viewpoint of thruster life if the propellant is purified from oxidizing components (see below), because the limits imposed by spacecraft contamination cannot be stated generally. Anode erosion may be manageable, as long as uniform (spotless) attachment is achieved.

Electrode losses (notably on the anode) dominate the efficiency limits of small MPD thrusters, where the electrode losses can take up 50 to 60% of the overall voltage drop. For larger thrusters (MW regime) this loss is probably less dominant (extrapolated from pulsed SF-MPD data), but it does strictly limit the current densities on anodes if simple radiation cooling is required.

MPD Thruster Cathode . Cathodes made of refractory metals (W, Ta) are at present the only ones known to be potentially suitable for larger MPD thrusters, where the so-called high current regime from a few hundred ampere into the high kiloamperes and gas pressures at the cathode from a few hundred millibar on down is applicable.

Cathodes of continuous thrusters can operate, in their design range of conditions, with an apparently spot-free diffuse arc attachment covering a fairly large area. To reach this optimal (from the viewpoint of erosion) condition, the cathode must be of the right material (e.g. thoriated tungsten), be able to reach the required temperature (2,600 - 3,300 K) over a sufficient area (implying adequate but not excessive cooling) and be surrounded with sufficient gas density for the imposed current. Under all other conditions, such as continuous thrusters during warm-up, cathodes with inadequate gas pressure or design or “aged” material (thoria depletion) as well as cold cathodes, pulsed thrusters operate in some form of spot mode. This involves local melting and substantial vaporization of cathode material, as will be discussed.

Thoriated tungsten cathodes can operate in the spot-free thermionic mode, with current densities up to at least 2 kA/cm2 with minimal losses, at (2,800 K, the highest still acceptable surface temperature from the viewpoint of vapor pressure [50, 57].

Much higher current densities (to at least 5 kA/cm2) are possible, but at excessive temperatures for long life (i.e. above 3,000 K) because of high sublimation rates. Aging of the material (presumably thoria depletion) was found to be a serious problem in some cases. [29]. For a detailed discussion see [30, 26].

At high current densities *within* the cathode, the Ohmic heating gives rise to severe problems. Cracks releasing molten material from the interior near to the rear end of the cathode, behind the arc attachment zone. Fig. 8 depicts a cathode of the DT2 thruster with a diameter of 16 mm which failed at a current level of 6500 A.

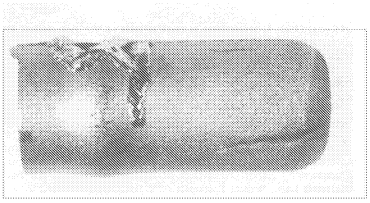

Fig. 8 Damaged cathode of DT2
(16 mm ∅, 6500A)

Investigations [26] lead to the conclusion that at the high temperatures inside the cathode the thoria lumps together, forming spheres of ThO_2, which reduce the conducting cross section of the cathode and hence further rising the temperature due to Ohmic heating until the thoria evaporates under destruction of the cathode (This was the reason for the tapered cathode design of the ZT3 thruster, Fig. 6).

Thruster anode. In a long arc without axial flow, there is a small ion drift (i.e. positive ion current) away from the anode. These ions must be replaced at the anode to provide plasma (space charge) neutralization and thus allow the main electron current to reach the anode. To produce these ions, either from ambient neutral atoms or from anode material, an anode arc contraction and fall zone sets itself up having, at the lower densities, a voltage close to the ionization potential of the substance to be ionized.

Spot-free anode functioning is, however, possible in SF-MPD thrusters. There the plasma is generated mostly near the cathode and in some cases also in the midstream discharge and is blown toward the anode surface. Under these conditions there is normally no need for ion generation near the anode and the anode potential drop becomes zero or even negative as predicted by the classical anode theory for this case. Anode phenomena are discussed in more detail in [21].

Electrode Erosion. The limits of allowable electrode erosion will first of all be set by thruster life requirements.

The allowable erosion, from the viewpoint of thruster life, depends on the life requirements - typically 1,000 to 10,000 hours for near-earth missions - and the thruster design, type and size. Some typical numbers for a 10-N continuous radiation cooled self-field thruster

(4kA, 1 g/s argon) for 3,000 hours life (consuming 4.3 · 10^{10} C, 11,000 kg propellant) would be:

	cathode (W)	*anode (Mo)*
allowable erosion mass loss m_{er}, (g)	50	250
m_{er}/Coulomb, (g/C)	1.2 . 10-3	5.8 . 10-3
m_{er}/propellant mass	4.6 . 10-6	2.3 . 10-5

This corresponds to a few millimeters per year (or the order of 10^{-7} mm/s) material loss from the faces of the electrodes exposed to the arc for that size and type of thruster. This is about or less than the normal vaporization rate of tungsten at 3,000 K, and 1/2,000th of that rate at the melting point.
The possible erosion mechanisms for both cathodes and anodes are

- macro particle ejection (spitting) and massive vaporization (boiling) from molten pools under macrospots,
- localized vaporization (boiling) at microspots,
- vaporization from larger molten surface areas (without boiling or spots),
- sputtering due to ion impact (normally negligible),
- continuous surface vapor loss due to excessive average surface temperature without melting.

With brittle metals (e.g. tungsten) there is, in addition, the possibility of cracking due to thermal fatigue.

Cathode erosion. In a steady-state MPD device one has to discern between two operation regimes:

- The ignition phase, which lasts typically about one second (depending on the ignition current and cathode mass and design)
- The steady operating phase, which lasts (at least in the laboratory) between several minutes to several hours.

The ignition phase is characterized by a cold cathode and a highly instable, spotty arc attachment. These arc spots jump irregularly over the cathode surface, causing melting with relatively high erosion and leaving "craters" of sizes ranging from some microns to a tenth of a millimeter. This starting phase ends when the cathode is hot enough for the thermionic emission to support the current demand. The measured averaged erosion during this phase is ca. 13 µg/s [26] and is insensitive to the propellant gas.
Contrary to the erosion during the ignition phase, the erosion in the thermionic phase [26] is dependant to the propellant: nitrogen yields the lowest (ca. 0.5 ng/C), Hydrogen the highest (ca. 2.2 ng/C) with argon in between (ca. 1.5 ng/C). It showed that the steady state erosion is very sensitive to the grade of the propellant: the cited values were reached with high grade gases, which were further cleaned from oxygen and humidity. With normal uncleaned welding argon, the erosion yields were about a factor 20 higher.
With a pure thermionic emission, erosion is dominated by the sublimation rate *s*, which can be calculated with the Dushman equation.

Anode erosion. Continuous self-field thrusters must be operated at currents some safe margin below the onset of instabilities or anode voltage rise regime, to avoid rapid destruction.
Anode erosion appears manageable with diffuse attachment (i.e. far from onset conditions) and possibly also with spots in pulsed and/or axial applied-field thrusters, using high melting metals.

Propellant Choice. The propellant choice affects the thruster, the system, the spacecraft, the atmosphere environment and the operating logistics. If the thermal thrust portion is not taken into account, the thrust to power ratio seemed to favor heavy propellants like argon, but also lighter mixtures like N_2H_4 and NH_3 have been taken into account, which also are storable and may be logistically (N_2H_4) the most desirable with still fair thrust to power ratios. Further thruster tests and system/mission studies are needed for final choices.
Liquid metals such as Li, K, In and others, have great advantages concerning storage, cooling capacities, ionization potential but will probably be ruled out because of contamination of the spacecraft by condensing and depositing of propellant on cool parts of the spacecraft.
For storage weight and volume, the highly cryogenic, low density propellant hydrogen is of course the worst. Hydrogen may be acceptable for missions requiring more or less continuous propellant use from the beginning, sufficient that the boil-off keeps the rest cold enough and can be used as propellant. In the longer future, hydrogen may be produced in space from water (where the oxygen is needed also) or from same other compound.

3.2 Magnetoplasmadynamic Thruster with Coaxial Applied Field

In this type of applied-field thruster, the electrodes are arranged coaxially like in an MPD self-field thruster; there is a nozzle-shaped [32] and a cylindrical (Fig. 9) type. By means of a coil or with permanent magnets, an axial, diverging magnetic field B_f is produced as shown in Fig. 9. Here the magnetic field interacts with the induced, azimuthal flow which can be explained with the Hall effect:

The z-component B_{fz} of the applied magnetic field causes a ring current j_θ in the direction of θ due to the radial current density component j_r according to the Hall term in Ohm's Law. This ring current, also called Hall current, in turn interacts with the magnetic filed and produces with the component B_{fr} an accelerating force in the direction of the flow and together with the component B_{fz} causes the pressure to rise on the thruster axis (pinch effect).
The formation of these Hall currents is therefore a prerequisite for propellant acceleration in these devices.

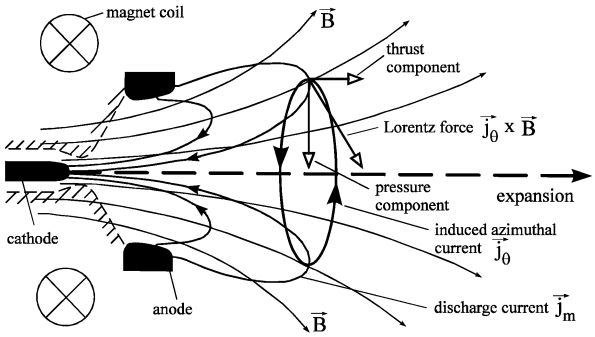

Fig. 9. Principle of an applied-field thruster with a coaxial field

The ring current can only form if the individual particles seldom collide. A characteristic parameter for these thrusters is therefore the so-called Hall parameter $\omega_e\tau_e$; here ω_e is the gyration frequency and τ_e the mean free flight time of the electrons. The Hall parameter is therefore the ratio of the gyration frequency of the electrons to their collision frequency. The higher the gyration frequency and the lower the collision frequency, the better an azimuthal current can form. That is why the Hall parameter must be as large as possible; in any case much larger than one.

Current Distribution. The magnetic field in coaxial applied-field thrusters is so large that due to the Hall effect, the electrical conductivity is clearly reduced perpendicular to the magnetic field which results in the transport of the current being hindered. Therefore the current stream lines are extended far outside the thruster. The influence of the applied magnetic field is therefore also called "magnetic nozzle".

The discharge current, whose distribution is a function of $\omega_e\tau_e$ bulges out far downstream as increases. This suggests the important influence of ambient pressure. [34]. Environmental influence on the overall process (participation of ambient gas) is given, leading to an uncertainty of thrust and particularly I_{sp} determination. Even with condensable propellants this effect can not be avoided reliably per ground testing because of the wide extension of the plume and the normally moderate dimensions of the vacuum facility.

Rotation of the Plasma. The components of the electrical field which are perpendicular to the magnetic field cause a plasma flow in the direction $\vec{E}_s \times \vec{B}$. For the applied-field thruster with a coaxial magnetic field this means that the plasma begins to rotate. The size of the moment of momentum D can be calculated as a closed integral without knowing the current density distribution [37]. In several experiments, circulating current spokes were observed and their frequency was measured [33].

Thrust. The thrust of an applied-field MPD device increases significantly with the magnetic field (Fig. 10). It is not possible to derive a simple equation for this dependency as with self-field thrusters. The thrust in an MPD thruster with a coaxial applied field essentially has four sources:

-The heating of the gas and expansion through a nozzle (dynamic effect on the material walls like an arcjet). -> $F_{therm.}$

-The discharge current crossing the magnetic field simultaneously results in an azimuthal force component that puts the plasma into rotation, which is considered an important source of energy addition. This energy can be partly converted into thrust energy. -> F_{swirl}

-As the discharge current crosses the applied magnetic field, azimuthal currents are induced that yield axial and radial Lorentz (j x B) forces, of which the axial component directly accelerates the plasma while the radial component confines the plasma and builds up a pressure hill, respectively. This energy again can be partly converted into thrust energy. -> F_{Hall}

-The interaction between the radial component of the primary current and the induced azimuthal magnetic field gives a self-magnetic acceleration. This plays only a subordinate role in applied-field thrusters. -> F_{self}

The total thrust can be calculated as the sum of these thrust components $F_{tot} = F_{Hall} + F_{swirl} + F_{therm} + F_{self}$

Whether this simple algorithm is applicable depends, however, on the definition of thrust portions. Quantifying each portion as being generated by total conversion of attributed energy added (e.g. $F_{swirl}=\int_V (j_r B_z u_\theta) dV$) to useful (axial) velocity, the following dependency is obtained under simplifying assumptions [38]:

$$F = [(F_{hall} + F_{self})/2] + \{[(F_{hall} + F_{self})/2]^2 + F^2_{swirl} + F^2_{therm}\}^{1/2} \quad (2)$$

Using this formula, one can estimate the order of magnitude of the maximum effect produced by each mechanism. Which mechanism prevails in thrust production depends on the selection of operating parameters and thruster geometry. In Table 2 below, a comparison is made between the electromagnetic thrust portions for different cases of B, I, and $\dot{m}$ that proves this statement. There is evidence that Joule heating and swirl production are energetically most relevant in the AF-MPD, with a substantial portion of the conversion taking place in the magnetic nozzle.

The discharge current-equivalent mass flow $\dot{m}_{equ} = (m_i / e) I$ (single ionization) where m_i is the ion mass, is far from being reached in known experiments [42, 38] except in rare cases of light propellants.

In the ideal case of energy gain and conversion under special consideration of rotational energy, voltage U (with a consequence to thrust F) should relate

quadratically with the magnetic field strength B as a result of back electromotive force (EMF) produced by azimuthal velocities. This dependency is not found in the experimental results [40], see also Eq. (3), which is proof that those energy processes are connected with inherent losses. There are different hypotheses used to explain non-ideal performance. One is that plasma viscosity plays an important role, hindering development of ideal azimuthal velocities by friction on outer (anode) walls, with velocity conversion in addition being limited by anomalous conductivity effects. [41] Plasma turbulence and anomalous diffusion certainly have a substantial influence, which leads to very moderate effective $\omega_e\tau_e$ [35].

Table 2. Operation conditions and calculated thrust components of some AF-MPD thrusters [44].

Thruster	Univ. Tokyo	Los Alamos
B [T]	0.10	0.19
$\dot{m}$ [kg/s]	$9\ 10^{-7}$	$2.5\ 10^{-5}$
I [A]	200	350
F_{hall}[N]	$4.4\ 10^{-2}$	$1.8\ 10^{-2}$
F_{swirl}[N]	$1.4\ 10^{-2}$	$6.9\ 10^{-1}$
F_{self}[N]	$1\ 10^{-4}$	$9\ 10^{-3}$

Thrust and discharge voltage generally tend to rise with the strength of the magnetic field and the discharge current [35],

$$F \text{ and } U_{tot} \sim I^{0.8\text{-}1}\ B_0^{0.5\text{-}1}\ ; \qquad (3)$$

see Fig. 10 for thrust.

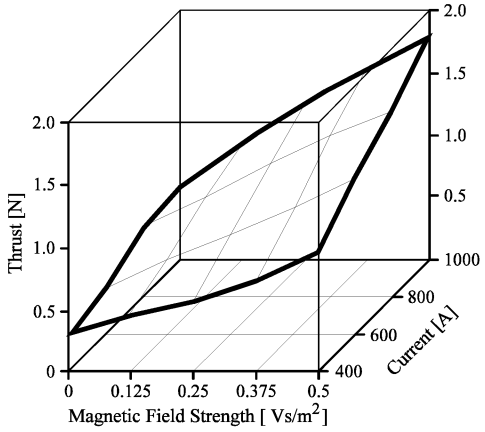

Fig. 10 Thrust as a function of discharge current and magnetic field strength (elevated power of laboratory type X-9, 100 mg/s argon, pa = 3.0 Pa)

As a consequence, for AF-MPD acceleration to be effective, at least a strong magnetic field (B) of adequate shape, an optimal degree of ionization to ensure good coupling of mass to electromagnetic effects, and moderate particle density in the discharge region are required.

Applicable Propellants. The magnetic thrust of an applied-field thruster essentially depends on the formation of Hall currents and for this a Hall parameter as large as possible is necessary. The Hall parameter is, however, independent of the propellant. Therefore, it imposes no additional criteria on the propellant choice.
In view of the need for a high degree of ionization at moderate losses, certain propellants suitable for AF-

MPD engines can be considered. These are preferably easy to ionize monatomic elements (with preferred materials underscored): noble gases (He, Ne, Ar, (Xe)) and alkali metals (Li] (Na, K)), but H_2, N_2, and N-H combinations have also been used, e.g., Refs. [38, 40], which suggests the capability of operating parallel to auxiliary chemical systems. The application of alkali metals is combined with considerable feed system problems and the danger of S/C contamination; the attainable tank pressure, however, is low in laboratory tests using condensable propellants that have a self pumping effect.

Thruster Developments. Applied-field thrusters with coaxial fields were developed in the USA, Germany, and the USSR in the 1960s and 1970s for power levels between 1kw-30kW The strength of the magnetic field was between .1 T and several T. Averaged exit velocities of approximately 40 km/s at efficiencies of up to 40% were achieved (the power to produce the magnetic field is not included in the calculation). Most of the development projects were terminated in the middle of the 1970s, with the exception of the USSR and some laboratories in the USA where limited work has been continued.

The typical average data for laboratory devices run at different locations are:
discharge current (I) = 100-200 (-1500) A; applied field (maximum) (B_0) = 0.05-1.0Vs/m^2; propellant mass flow ($\dot{m}$) = 5-50 mg/s Ar, Li (He, Kr, Xe, H_2, N_2, NH_3); ambient pressure (p_a) = 10-0.05 (- 10^{-4}) Pa; discharge voltage (U) = (50 -) 100-150 V; thrust (F) = 200-2000 mN; specific impulse (I_{sp}) = F/$\dot{m}$ = 15 - >35 km/s; and thrust efficiency (η_T) = F/(2 $\dot{m}$ U–I) = <20 - 40%. Efficiencies are reported as tending to be low for gaseous propellants, in particular argon (which has been used for the majority of tests), in contrast to alkali propellants, especially lithium.
The radiation cooled applied-field accelerator DFVLR-X16 developed at DLR in the early 70s, in which the magnetic field is produced by means of a coil, is from today's point of view one of the best devices. At the same time, NASA was examining a thruster with a superconductive magnet. Both of these devices and the results achieved are discussed here as examples of this technology.
Today, applied-field thrusters are once again being investigated in Japan, the USA Germany and Italy.

Thruster X-16 from DLR Stuttgart. The thruster X-16 (Fig. 11) is equipped with a radiation-cooled anode and a hollow cathode. This device was able to achieve a thrust of 251 mN with a magnetic field of 0.6 T at a current of 80 A and a voltage of 145 V with 7 mg/s argon mass flow rate [35]. This is equal to an effective exit velocity of approximately 36 km/s at an efficiency of 38.8%.

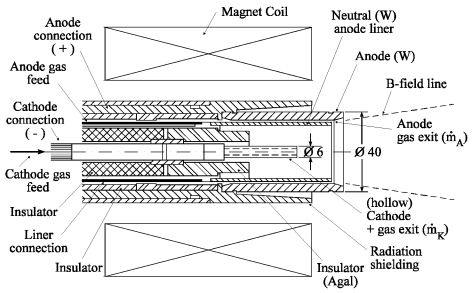

Fig. 11 Applied-field thruster X-16 from DLR Stuttgart. [35]

NASA thruster with superconductive magnet. Among others, a radiation-cooled thruster with a superconductive magnet was tested at the NASA Lewis Research Center).

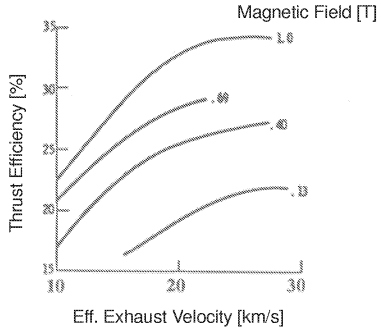

Fig. 12. Dependence of the efficiency on the effective exit velocity with different magnetic fields using a thruster with a superconductive magnet [32].

One can see from Fig. 12 that compared to self-field thrusters, the efficiency can only be significantly improved when the strength of the magnetic fields is distinctly larger than 0.1 T. This means that the effort of producing the magnetic field, which is not taken into account in calculating the efficiency, seems to be only justifiable with stronger magnetic fields.

Thruster developments in Russia. For several decades the Moscow Aviation Institute has been investigating applied-field thrusters with lithium as propellant up to a performance level of approximately 150 kW. A sketch of this device is shown in Fig. 13. The cathode consists of a bundle of hollow cathodes. The tungsten anode is radiation-cooled. At relatively low magnetic field strength, (0.075 < Bf < 0.09 T), a thrust of ca 4.5 N was achieved at a current of ca 2.9 kA and a mass flow rate of 107 mg/s. This is equivalent to an effective exhaust velocity of ca 42 km/s. The efficiency was ca 48% [6].

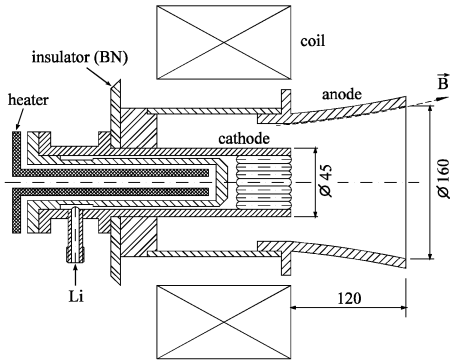

Fig. 13: Applied-field thruster with lithium as propellant up to ca 150 kW.

Necessary Test Facilities. When testing applied-field thrusters in a laboratory, one must keep in mind that compared to self-field thrusters the current distribution extends quite far outside of the device. However, interaction with the wall of the test container must be precluded. This means that the tank must be made of non-magnetic steel. Due to the interaction of the discharge with the residual gas, surrounding gas may be sucked in near the anode if the tank pressure is too high. Therefore, pressures lower than 10^{-3} mbar are required. Currently there are no facilities available for testing thrusters at high electric power levels (higher than 100 kW).

4. HIGH POWER HYBRID THRUSTER CONCEPT ATTILA

Among the hybrid thrusters currently being investigated, only the concept ATTILA promises a thrust density high enough so that high thrusts can be expected. The high power hybrid thruster ATTILA (see Fig. 14), which is under construction at IRS, consists of two stages: a thermal arcjet section is followed by an induction stage. The plasma jet generated by the thermal arcjet section, which is operated in a power range between 50 to about 100 kW, is injected into a ceramic tube which is surrounded by a magnetic coil. In this stage additional energy is added by inductive heating prior to the expansion in the nozzle [8]. In the inductive second stage the energy is coupled near the surface owing to the skin-effect. In this way the temperature of the thermal arcjet's cold gas casing can be increased considerably and ultimately a significantly higher exit velocity can be achieved. In preliminary tests this effect

has already been proven by means of a baffle plate for force measurements.

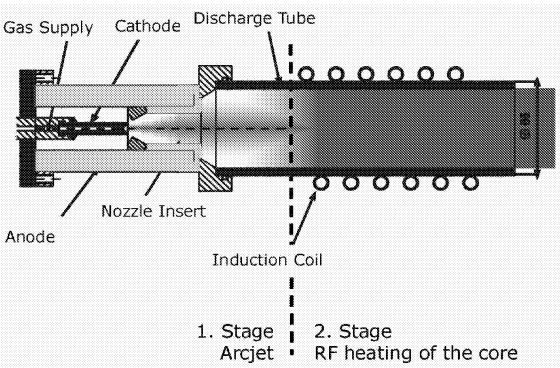

Fig. 14. Hybrid plasma generator.

5. SUMMARY

Promising candidates for heavy payloads in space propulsion are different plasma propulsion systems. Electrothermal arcjets cover a wide range of input power, from several 100 W to several 100 kW. Low power devices have been implemented in commercial applications with hydrazine as propellant because of its rather evolutionary step in specific impulse compared to the well established chemical thrusters and its simplicity, reliability and low system mass compared to other electric propulsion systems. This technology has been investigated so far up to 100 kW power on a laboratory level and the results are very promising. With hydrogen as propellant exit velocities could be achieved over 20 km/s and there is hope to further increase this value by increasing the power level and optimizing the design. High thrust levels of 25 N have already been achieved in the laboratory with stationary self-field MPD thrusters with argon as propellant, but so far plasma instabilities limit the exit velocity to 15 km/s for various investigated propellants including hydrogen. These instabilities have been intensively investigated and there is hope to increase specific impulse by changing the thruster geometry. High exit velocities of 40 km/s and 4.5 N thrust have been achieved with an applied filed MPD device with lithium as propellant. But there are some disadvantages: thrust density is lower by one decade compared to the other two plasma sources, the performance is not demonstrated so far with non-contaminating propellants in stationary operation at high power levels and much lower tank pressure is required for the investigation of applied-field devices. A hybrid thruster, consisting of an electrothermal arcjet as a first stage combined with an inductive RF-stage offers the possibility to not only increase the exit velocity but also the thrust density. Preliminary laboratory tests look promising.

6. REFERENCES

1. Schmidt, T., Seboldt, W., Auweter-Kurtz, M. , Propulsion Options for Manned Mars Missions, 16_333_P, 6th International Symposium, Propulsion for Space Transportation of the XXIst Century, Versailles, Frankreich, May 2002.
2. Shoji, J.M., Solar Rocket Component Study, AFRPL-TR-84-057, 1984.
3. Farbman, G., Upgraded Nerva Systems: Enabler Nuclear System, in: NASA Conference Publication 10079, Nuclear Thermal Propulsion, Cleveland 1991.
4. Auweter-Kurtz, M., Gölz, T., Habiger, H., Hammer, F., Kurtz, H., Riehle, M., Sleziona, C., High Power Hydrogen Arcjet Thrusters, Journal of Propulsion and Power, Vol. 14, No. 5, September-October 1998, pp. 764-773.
5. Wegmann, T., Experimentelle Untersuchung kontinuierlich betriebener magnetoplasma-dynamischer Eigenfeldtriebwerke, Dissertation, Institut für Raumfahrtsysteme, Universität Stuttgart, 1994.
6. Tikhonov, V., Semenikhin, S., Brophy, J.R., Polk, J.E., The Experimental Performances of the 100 kW Li MPD Thruster with an External Magnetic Field, Proc. Of the 24th IEPC, Moscow, Russia, 1995
7. Christensen, J.A., et al., Design and Fabrication of a Flight Model 2.3 kW Ion Thruster for the Deep Space 1 Mission, AIAA-98-3327, 34th AIAA/ASME/SAE/-ASEE Joint Propulsion Conference, Reston, VA, July 1998.
8. Laure, S., Boehrk, H., Auweter-Kurtz, M., Design Optimization of the Hybrid Plasma Generator System – ATTILA, 4th Int. Symp. On Applied Plasma Science, Kyoto, Japan, Sept. 2003.
9.Chavers, G., Chang-Diaz, F., Momentum and Heat Flux Measurements in the Exhaust of VASIMR Using Helium Propellant, IEPC-28, Proc. of the 28th IEPC, Toulouse, France, March 2003.
10. Archipov, B:A., Bober, A.S., Gnizdorr, R.Y., et al., The Results of 7000-hour SPT 100 Life Testing, IEPC-95-39, Proc. of the 24th IEPC, Moscow, Russia, 1995
11. Kurtz, H., Arcjet Thrusters, Final Report – Propulsion 2000, IB-00-06a, Institut für Raumfahrtsysteme, Universität Stuttgart, 2000.
12. Curran, F., Caveny, L., Hydrogen Arcjet Technology Status, IEPC-93-215, Seattle, WA, 1993.
13. PRIMEX Aerospace Company, Space Systems Capabilities & Technologies, 99-H-2512A, Redmond, WA, 1999.
14. Bromaghin, D. et al., An Overview of the On-Orbit Results from the Electric Propulsion Space Experiment (ESEX), IEPC-99-182, Kitakyushu, Japan, 1999.
15. Butler, G., Cassady, R., Hoskins, W., King, D., Kull, A., Performance of Advanced Concept Hydrogen Arcjet Anodes, IEPC-93-211, Seattle, WA, 1993.

16. Aston, G., Aston, M.B. Integrated Design Arcjets for High Performance, IEPC-97-090, Cleveland, OH, 1997
17. G.L. Cann, State of the Art of Electromagnetic and Electrothermal Propulsion, Technion Inc., Report 07-040, prepared for Rockwell Int. Space Division, Irvine, CA, July 1977.
18. Maecker, H., Plasmaströmungen in Lichtbögen infolge eigenmagnetischer Kompression, Zeitschrift für Physik, Bd. 141, 1955, pp. 198 – 216.
19. Jahn, R.G.,Physics of Electric Propulsion, McGraw Hill Book Co., New York, 1968
20. Auweter-Kurtz, M., Boie, C., Kaeppeler, H.J., Kurtz, H.L., Schrade, H.O., Sleziona, P.C., Wagner, H.P., Wegmann, T., Magnetoplasmadynamic Thrusters: Design Criteria and Numerical Simulation, Int. J. of Applied Electromagnetics in Materials 4 (1994) pp. 383 – 401.
21. Hügel, H., Zur Funktionsweise der Anode im Eigenfeldbeschleuniger, DFVLR-FB 80-30, 1980.
22. Schrade, H.O., Rösgen, T., Wegmann, T., The Onset Phenomena Explained by Run-Away Joule Heating, IEPC-91-022, 22nd IEPC, Viareggio, Italy, 1991.
23. Rudolph, L.K., The MPD Thruster Onset Current Performance Limitation, Ph.D. thesis, Nov. 1980, Princeton University, Princeton.
24. Lawless, J.L., Subramanian, V.V. A Theory of Onset in MPD Thrusters, AFOSR Report 83-033, 1983.
25. Boyle, M.J., Clark, K.E., John, R.G., Flowfield Characteristics and Performance Limitations of Quasi-Steady Magnetoplasmadynamic Accelerators, AIAA Journal, Val. 14, No. 7, July 1976.
26. Auweter-Kurtz, M., Glocker, B., Kurtz, H.L., Loesener, O., Schrade, H.O., Tubanos, N., Wegmann, T., Willer, D., Polk, J.E., "Cathode Phenomena in Plasma Thrusters", Journal of Propulsion and Power, Vol. 9, No. 6, Nov.-Dec. 1993, pp. 882-888.
27. Wagner, H.P., Kaeppeler, H.J., Auweter-Kurtz, M., Instabilities in MPD thruster flows: 1. Space charge instabilities in unbounded and inhomogeneous plasmas, J. Phys. D: Appl. Phys., 31, (1998) pp. 519-528.
28. Heiermann, J. Ein Finite-Volumen-Verfahren zur Lösung magnetoplasmadynamischer Erhaltungsgleichungen, Dissertation, Institut für Raumfahrtsysteme, Universität Stuttgart, 2002.
29. Malliaris, A.C., Phenomena in the Cathode Region of an MPD Accelerator, AIAA Paper 67-47, 1967.
30. Goodfellow, K.D., A Theoretical and Experimental Investigation of Cathodes Processes in Electric Thrusters, Ph. D. thesis, University of Southern California, Los Angeles, 1966. Also: JPL internal Doc. JPL D-13969, 1996
31. Hügel, H. and Krülle, G., Phänomenologie und Energiebilanz von Lichtbogenkathoden bei niedrigen Drucken und hohen Stromstärken, Beiträge aus der Plasmaphysik, Bd. 9, pp. 87-116, 1969.
32. Seikel, G.R., York, T.M., Condit, W.C., Roles for Magnetic Thrusters in Orbit-Raising Missions, SeiTec-Report 8203, SeiTec, Cleveland, OH, 1982.
33. Schock, W., Zur Verteilung der elektrischen Stromdichte in Magneto-Plasma-Dynamischen (MPD)-Beschleunigern, Dissertation, Universität Stuttgart, 1974.
34. Connolly, D.J. and Sovie, R.J., Effect on Background Pressure on Magnetoplasmadynamic Thruster Operation, Journal of Spacecraft and Rockets Vol. 7, No. 3, 1970, p. 255.
35. Krülle, G., Zur Dynamik des axialsymmetrischen magnetoplasmadynamischen Beschleunigers (MPD-Triebwerk) mit überlagertem Magnetfeld, Dissertation, Technische Universität München, 1974.
36. Tanaka, M. and Kimura, I., Current Distribution and Plasma Acceleration in MPD Arcjets with Applied Magnetic Fields, Journal of Propulsion Vol. 4, No. 5, 1988
37. Cann, G.L., Harder, R.L., Moore, R.A., Lenn, P.D., Hall Current Accelerator, NASA CR-54705, 1966.
38. Arakawa, Y. and Sasoh, A., Electromagnetic Effects in an Applied Field Magnetoplasmadynamic Thruster, Journal of Propulsion & Power Vol. 8, No. 1, 1992, p. 98.
39. Bishop, A.R., Connolly, D.J. and Seikel, G.R., Test of Permanent Magnet and Superconducting Magnet MPD Thrusters, AIAA Paper 71-696, 1971.
40. Myers, R.M., Applied Field MPD Thruster Performance with Hydrogen and Argon Propellants, *Journal of Propulsion & Power,* Vol. 9, No. 5, 1993, p. 781.
41. Mikellides, P.G., Turchi, P.J., Roderick, N.F., Theoretical Model for Applied Field MPD Thrusters, AIAA-95-2676, July 1995.
42. Kruelle, G. and Zeyfang, E., Preliminary Conclusions of Continuous Applied Field Electromagnetic Thruster Research at DFVLR, AIAA Paper 75-417, 1975.
43. Kruelle, G., Characteristics and Local Analysis of MPD Thruster Operation, AIAA Paper 67-672, 1967.
44. Sasoh, A. and Arakawa, Y., Thrust Formula for an Applied-Field MPD Thruster Derived from Energy Conservation Equation, IEPC 91-062, 1991
45.Krülle, G., Auweter-Kurtz, M., Sasoh, A., Technology and Application Aspects of Applied Field Magnetoplasmadynamic Propulsion, Journal of Propulsion and Power, Vol. 14, No. 5, 1998, pp. 754-763.